

# Decoupled MPPI-Based Multi-Arm Motion Planning

Dan Evron<sup>1</sup>, Elias Goldsztejn<sup>2</sup>, Ronen I. Brafman<sup>3</sup>

**Abstract**—Recent advances in sampling-based motion planning algorithms for high DOF arms leverage GPUs to provide SOTA performance. These algorithms can be used to control multiple arms jointly, but this approach scales poorly. To address this, we extend STORM, a sampling-based model-predictive-control (MPC) motion planning algorithm, to handle multiple robots in a distributed fashion. First, we modify STORM to handle dynamic obstacles. Then, we let each arm compute its own motion plan prefix, which it shares with the other arms, which treat it as a dynamic obstacle. Finally, we add a dynamic priority scheme. The new algorithm, MR-STORM, demonstrates clear empirical advantages over SOTA algorithms when operating with both static and dynamic obstacles.

## I. INTRODUCTION

Motion planning is a key component in robotic systems. In this paper, we are particularly concerned with motion planning for multiple robots, and in particular, multiple high-DOF arms in dynamic settings. This problem arises in two-armed humanoid robots and on the factory floor, where, e.g., multiple arms may be used to place arriving items into respective boxes. In these applications, one must plan the path of each arm to its current target, which may constantly change or even require tracking, while ensuring that arms do not collide with each other and with additional potential static and dynamic objects, such as human co-workers.

There are multiple methods for solving multi-robot motion planning. Some existing methods [1], [2] provide optimality guarantees in some cases and under suitable assumptions. Others [3], [4] are more heuristic in nature. While all of these algorithms attempt to exploit the decoupled structure of the problem, almost all of them solve the problem *centrally*, i.e., jointly computing a path for all robots. This implies that a single coordinating machine must handle the entire large associated computational cost. This problem is further exacerbated given continuous tasks in which new tasks arrive while some arms are already executing a motion plan, as the entire plan for all arms must be re-evaluated. This often results in slow and non-responsive (or “laggy”) motion.

To address this problem, we seek a decentralized, reactive online algorithm that can adapt its path based on the current state of the other arms, and in which each arm computes its own path only. To achieve this, we build on STORM [5], a SOTA motion planner that uses GPUs to efficiently implement a parallel-sampling-based model-predictive control [6]

This research was supported by Ben-Gurion University of the Negev through the Agricultural, Biological and Cognitive Robotics Initiative (funded by the Marcus Endowment Fund and the Helmsley Charitable Trust).

<sup>1</sup> <sup>2</sup>, <sup>3</sup> The Department of Computer Science at Ben-Gurion University of the Negev. [evrond@post.bgu.ac.il](mailto:evrond@post.bgu.ac.il), [eliasgol@post.bgu.ac.il](mailto:eliasgol@post.bgu.ac.il), [brafman@bgu.ac.il](mailto:brafman@bgu.ac.il)

method. STORM naturally handles static obstacles, but is not designed to handle dynamic obstacles, such as additional arms. In principle, one can treat other arms as static obstacles, using their current position, and hope that with a sufficiently high sampling and replanning rate, they will avoid each other. Our empirical evaluation shows that this approach is unsafe and leads to many collisions.

Instead, we model the other arms as dynamic obstacles and modify the cost function used by STORM to account for both static and dynamic obstacles: Arms communicate a sparse representation of their near-term trajectory to each other and incorporate the received trajectories in their cost function. We show that this leads to dramatic improvements.

However, when multiple arms must reach or pass through similar regions to perform their task, if the cost of collisions with dynamic obstacles is low, the arms will likely collide. And if this cost is high, they will oscillate between attempting to reach the goal and evading each other. We address this using a distance-based priority scheme [7].

We evaluate our algorithm empirically in the Isaac-Sim simulator [8] on diverse tasks, demonstrating the impact of different components of the algorithm using ablation studies. We compare it with centralized and decentralized SOTA algorithms, showing its clear empirical advantage.

To summarize, our main contributions are: (1) MR-STORM, a state-of-the-art, fully decentralized, multi-robot motion planner tailored for complex multi-arm manipulation tasks in cluttered environments with uncertain dynamics. MR-STORM is implemented with high efficiency, incurring negligible runtime overhead relative to the control frequency of STORM. (2) A novel, fully decentralized prioritization scheme for coordinating multi-robot systems without centralized control. (3) Extensive experimental validation across 120 simulated scenarios, benchmarking MR-STORM against established baselines on realistic robot models with physical constraints. Code and experimental data are freely available at <https://roboworkshop.github.io/multi-robot-mpc/>.

## II. RELATED WORK

*a) Single-robot motion planning:* Given an initial configuration  $q_{\text{start}}$  and a goal  $q_{\text{goal}}$ , the motion-planning problem seeks a collision-free trajectory  $\xi$  in configuration space  $\mathcal{C}$  that satisfies kinematic/dynamic constraints while minimizing a task-specific cost (e.g., path length/time, smoothness, collision penalties). A central design choice is the *search space* and its representation: many planners build a discrete graph and run graph search; others optimize trajectories directly in continuous spaces.

Classical planners construct a discrete structure (uniform grids, visibility/Voronoi graphs, or *probabilistic roadmaps* [9]) and then apply Dijkstra, A\*, or D\* [10]–[12]. On finite graphs, they provide completeness and, with admissible heuristics, optimality guarantees. *RRT* [13] interleaves sampling and structure growth, expanding a tree toward random samples. Asymptotically optimal variants (PRM\*/RRT\*) recover optimal solutions as the number of samples increases [14].

Gradient-based methods (e.g., CHOMP, STOMP [15], [16]) optimize continuous trajectory parameterizations (splines or time-discretized waypoints). They produce smooth motions but may settle in local minima and typically require good initialization and differentiable surrogate costs.

MPC solves at each step for a finite-horizon control sequence  $\mathbf{u}_{0:H-1}$  using an approximate dynamics model and motion constraints, attempting to optimize some cost function. Only the first control  $u_0$  is executed before replanning (receding horizon). MPC naturally accommodates task-space objectives, smoothness/effort penalties, and hard/soft constraints (e.g., joint, velocity, workspace), and is reactive to changes in goals or obstacles due to frequent replanning.

Model predictive path integral (MPPI) and information-theoretic MPC draw  $N$  stochastic control sequences around a nominal  $\bar{\mathbf{u}}$ , roll out candidate trajectories under the approximate dynamics, evaluate total costs, and compute a control update via importance weighting (e.g., [6], [17], [18]).

Building on MPPI [6], STORM [5] targets robotic arms with manipulator-specific design: (i) signed-distance-field collision and self-collision costs; (ii) smoothness via acceleration/jerk penalties; (iii) joint/velocity limit handling via soft constraints; (iv) task-space objectives (pose tracking, waypointing); and (v) batched rollouts with approximate dynamics. STORM serves as an “off-the-shelf” low-latency trajectory optimizer for arms and has been integrated into modern stacks (e.g., [19]). It can support high control rates [19] and is widely regarded as state-of-the-art for *reactive* motion generation in high-DOF manipulators. Currently, it provides a coupled planner; in this work, we extend it to decoupled multi-arm planning.

As far as efficiency, graph/roadmap methods suffer most from the curse of dimensionality: the samples/vertices and neighborhood sizes needed to capture connectivity grow quickly with DOF growth, and nearest-neighbor plus collision queries dominate runtime [14], [20], [21]. Tree-based sampling avoids full-space discretization but still struggles in high-dimensional narrow passages and, in optimal variants, incurs extra rewiring/neighbor costs. Trajectory-optimization methods scale per iteration primarily with the number of time knots (via forward kinematics (FK)/collision/gradient evaluations) and are less sensitive to DOF but remain local. MPC/MPPI/STORM wall-clock depends mainly on horizon length and per-step evaluation; while FK and collision costs increase with DOF, parallel rollouts mitigate (but do not eliminate) dimensionality effects. This motivates our decoupled multi-arm approach that leverages per-arm planners while minimizing cross-arm search growth.

*b) Multi-robot motion planning.*: Let  $\mathcal{C}_i$  denote the configuration space of arm  $i$  and  $\mathcal{C} = \prod_{i=1}^M \mathcal{C}_i$  the composite space with pairwise self and cross collision constraints. A central design choice is whether to do *coupled* planning in  $\mathcal{C}$  or *decoupled* planning per arm in  $\mathcal{C}_i$  with some coordination. Classical search or sampling can be lifted to the composite space, yielding completeness and (in some cases) optimality on the induced discrete structure. Methods such as *dRRT\** [1] exploit implicit product roadmaps to avoid explicit construction, improving efficiency while preserving asymptotic guarantees; however, performance still degrades as the sum of DOFs grows and inter-robot constraints accumulate.

*Prioritized planning* [3], [22] assigns an order over arms: plan for arm 1, then for arm 2 while avoiding arm 1’s path, etc. Static priorities are simple but less reactive and sensitive to ordering; dynamic variants partially alleviate this by allowing priority changes on contention.

In decoupled planners, agents first generate individual plans, then *resolve conflicts*. *CBS*-style approaches [2] build a constraint tree over space–time conflicts, relying on per-arm low-level planners; hybrid variants (CBS-MP [23] /CBS-MPC [4]) substitute sampling-based low-level planning. These work well when interactions are sparse, but constraint sets can grow rapidly as trajectory overlaps increase, pushing the search toward coupled behavior.

Velocity-obstacle methods (e.g., ORCA [24]) and distributed MPC optimize locally per agent, often with limited communication. They are highly reactive but can enter deadlocks/livelocks in tight coupling unless augmented with arbitration or shared intent.

In this paper, we describe a decoupled algorithm that builds on the STORM algorithm, which is particularly intended for multi-arm motion planning, especially in constrained spaces. We adapt STORM/MPPI to the multi-arm setting by keeping *per-arm* receding-horizon planners and sharing *intention trajectories*. Other arms’ plans enter the MPPI cost via signed-distance penalties and time windows; a *dynamic prioritization* scheme arbitrates contention when multiple arms require similar workspace regions. This preserves STORM’s low latency and smoothness while enabling distributed coordination without full composite search.

### III. BACKGROUND

#### A. The formal motion-planning problem

Let  $\mathcal{C}$  be the configuration space of a robot,  $\mathcal{W}$  its workspace, and  $FK : \mathcal{C} \rightarrow \mathcal{W}$  the forward kinematics mapping. For a body  $b$  on the robot, let its pose be  $X^b \in SE(3) \equiv (p^b, q^b)$ . Obstacles occupy  $\mathcal{O} \subset \mathcal{W}$ , and the collision-free set is  $\mathcal{C}_{\text{free}} = \{q \in \mathcal{C} : FK(q) \cap \mathcal{O} = \emptyset\}$ . We use  $cd(b_1, b_2)$  to denote the distance between two bodies.

At control time  $t$ , given  $q_{\text{start}}, q_{\text{goal}} \in \mathcal{C}_{\text{free}}$ , the goal is to find a (possibly time-parameterized) trajectory  $\xi = \{q_0, \dots, q_T\}$  with  $q_0 = q_{\text{start}}$ ,  $q_T \approx q_{\text{goal}}$ , satisfying any motion constraints while minimizing the task cost. A

standard discrete objective is

$$J = \Phi(x_T) + \sum_{k=0}^{T-1} \ell(x_k, u_k) \quad (1)$$

s.t.  $x_{k+1} = f(x_k, u_k), \quad g(x_k, u_k) \leq 0$

where  $x_k$  denotes the system state, typically position and velocity,  $u_k$  is the control input,  $f$  is the true dynamics model,  $\ell$  aggregates running terms (path/time, smoothness, control effort), and  $g \leq 0$  encodes joint/velocity/ workspace limits and collision avoidance via  $cd(\cdot, \cdot)$  or signed-distance fields at (observable) horizon steps, and  $\Phi$  is the "cost-to-go" beyond horizon, i.e.,  $\Phi \approx \sum_{k=T}^{\infty} l_k$

For  $M$  arms with configuration spaces  $\{\mathcal{C}_i\}_{i=1}^M$ , the composite space is  $\mathcal{C} = \prod_{i=1}^M \mathcal{C}_i$ , with added inter-robot collision constraints  $cd(b_1^i, b_2^j) \geq 0$ . Coupled planners optimize in  $\mathcal{C}$ ; decoupled planners keep per-arm problems and coordinate their path in different ways. We build on the latter.

### B. STORM: sampling-based MPC (MPPI)

STORM [5] is a realization of model predictive path integral (MPPI) [6] tailored to manipulators: it supports non-differentiable collision costs via  $cd(\cdot, \cdot)$ , handles joint/velocity limits, and achieves low-latency receding-horizon control by parallel evaluation of  $N$  rollouts. It uses an approximate dynamics model  $\hat{f}(x, u)$  to sample trajectories, select the best one, and apply its first control input. More specifically, at control time  $t$ , STORM maintains a nominal control distribution along a horizon  $h \in \{0, \dots, H-1\}$  with mean and covariance  $\mu_{t,h}, \Sigma_{t,h}$ . It draws  $N$  sampled control sequences  $u_{t,h}^{(n)} = \mu_{t,h} + \varepsilon_{t,h}^{(n)}$ ,  $n = 1, \dots, N$ , where  $\varepsilon_{t,h}^{(n)} \sim \mathcal{N}(0, \Sigma_{t,h})$ . Each sampled sequence  $\{u_{t,0:H-1}^{(n)}\}$  is rolled out under the approximate dynamics  $\hat{f}$  to produce a trajectory. Its discounted cumulative cost  $\hat{C}_t^{(n)} = \hat{q}_{t,H-1,n} + \sum_{h=0}^{H-2} \gamma^h \hat{c}_{t,h,n}$  is computed, where  $\hat{c}_{t,h,n}$  is the per-step stage costs and  $\hat{q}_{t,H-1,n}$  is the terminal cost (a.k.a. cost-to-go). The executed control at time  $t$  is the first element of the lowest-cost sampled path.

Next, the sampling distributions are updated as follows: a weight is assigned to each trajectory:

$$w_t^{(n)} = \frac{\exp(-\hat{C}_t^{(n)}/\lambda)}{\sum_{m=1}^N \exp(-\hat{C}_t^{(m)}/\lambda)}. \quad (2)$$

$\lambda$  is the temperature hyper-parameter. Next, we compute

$$\tilde{\mu}_{t,h} = \sum_{n=1}^N w_t^{(n)} u_{t,h}^{(n)} \quad \tilde{\Sigma}_{t,h} = \sum_{n=1}^N w_t^{(n)} (u_{t,h}^{(n)} - \tilde{\mu}_{t,h})(u_{t,h}^{(n)} - \tilde{\mu}_{t,h})^\top \quad (3)$$

Finally, these are used to update the distributions using an exponential moving averages with step sizes  $\alpha_\mu, \alpha_\Sigma \in (0, 1]$ :

$$\begin{aligned} \mu_{t+1,h} &\leftarrow (1 - \alpha_\mu) \mu_{t,h} + \alpha_\mu \tilde{\mu}_{t,h}, \\ \Sigma_{t+1,h} &\leftarrow (1 - \alpha_\Sigma) \Sigma_{t,h} + \alpha_\Sigma \tilde{\Sigma}_{t,h}. \end{aligned} \quad (4)$$

After this, the horizon is shifted (receding horizon) and the process repeats at  $t+1$ , "hot-starting" from the previous step ( $t$ ) solution.

A key element of STORM is its cost function. Let  $X^{ee}$  be the end-effector pose,  $X^g$  a goal/waypoint pose in the world, and  $S = \{s_1, \dots, s_J\}$  collision spheres attached to links. Along each rollout we obtain poses  $\hat{X}_{t,h,n}^b = \text{FK}^b(\hat{q}_{t,h,n})$  via forward kinematics FK. A typical stage cost (for the single-robot planning problem) is

$$\begin{aligned} \hat{c}_{t,h,n} = w_p &\underbrace{\hat{c}_{\text{pose}}(\hat{X}_{t,h,n}^{ee}, X_t^g)}_{\text{goal reaching}} + w_s \underbrace{\hat{c}_{\text{stop}}(\dot{q}_{t,h,n})}_{\text{stopping}} \\ &+ w_j \underbrace{\hat{c}_{\text{joint}}(\hat{q}_{t,h,n})}_{\text{joint limit avoidance}} + w_m \underbrace{\hat{c}_{\text{manip}}(\hat{q}_{t,h,n})}_{\text{avoid singularities}} \\ &+ w_c \underbrace{(\hat{c}_{\text{coll}}(\hat{q}_{t,h,n}, \mathcal{O}) + \hat{c}_{\text{self-coll}}(\hat{q}_{t,h,n}))}_{\text{environment \& self collision}} \end{aligned} \quad (5)$$

where the different weight terms  $w_* \geq 0$ . Here:

- $\hat{c}_{\text{pose}}(X^{ee}, X^g)$  penalizes the distance and orientation error between end-effector and goal.
- $\hat{c}_{\text{stop}}(\dot{q})$  penalizes any step in the horizon where the joint velocity exceeds the limit needed to guarantee a safe stop in reaction to unexpected events at the end of the horizon.
- $\hat{c}_{\text{joint}}(q)$  penalizes joint configurations outside safe limits with a threshold buffer.
- $\hat{c}_{\text{manip}}(q)$  penalizes states with small "manipulability" (estimated by the volume of the ellipsoid formed by the robot's kinematic Jacobian matrix), encouraging motions that avoid kinematic singularities.
- $\hat{c}_{\text{coll}}, \hat{c}_{\text{self-coll}}$  penalize for environment collision (distance from objects) and self-collision. Note that STORM's dynamics model does **not** take into account trajectories of objects, i.e.  $\forall h \in 1, \dots, H-1, \forall o \in \mathcal{O} : \hat{X}_{t,h}^o = X_t^o$ .

### IV. DECOUPLED STORM FOR MULTI-ARM MP

We now describe MR-STORM, a multi-arm/robot decoupled variant of STORM. MR-STORM modifies STORM to take into account dynamic obstacles by adding a cost term that penalizes collision with them and uses their anticipated positions during the horizon  $H$ . Each arm runs STORM using the modified cost function, executes the first action, and transmits information about its plan to the other arms, which use it in their cost function in the next step. We also add a dynamic prioritization scheme to prevent deadlocks.

#### A. Handling Dynamic Obstacles

In vanilla STORM, collision checking is performed solely against the robot's predicted trajectories, obtained from rollouts, treating obstacles as if they are static. To address dynamic obstacles, we modify the cost function to reflect collisions with them. Hence, we add a new term to STORM's cost function penalizing collisions with dynamic obstacles using their estimated trajectories. More specifically, let  $a^{(i)} \in \mathcal{A}$  be the  $i$ -th arm (or any type of robot) and  $o \in \mathcal{O}$  be an obstacle. Recall that  $cd(\cdot, \cdot)$  defines the Euclidean distance between body surfaces. MR-STORM's cost function for  $a^{(i)}$  is defined as:

$$\hat{c}_{t,h,n}^{(i)} = \hat{c}_{t,h,n} + w_d \hat{c}_{dyn_{t,h,n}} \quad (6)$$

where  $w_d \hat{c}_{dyn}$  is added to eq.5. We define:

$$\hat{c}_{dyn_{t,h,n}}^{(i)} := \sum_{o \in \mathcal{O}} f_{mask}(cd(\hat{a}_{t,h,n}^{(i)}, \hat{o}_{t,h,n}), B)$$

with

$$f_{mask}(x, B) := \text{Relu}(1 - \frac{x}{B})$$

Recall that  $\text{Relu}(x) = x$  when  $x > 0$  and is 0 otherwise. Since STORM models each arm  $a$  as a set of spheres  $S$ , we have:

$$cd(\hat{a}_{t,h,n}^{(i)}, \hat{o}_{t,h,n}) \equiv \min_{1 \leq k < |S_i|} cd(\hat{s}_{t,h,n}^{(i,k)}, \hat{o}_{t,h,n}), B)$$

Here,  $s^{(i,k)}$  is the  $k$ -th sphere of arm  $i$ .  $B$  is a hyperparameter that specifies the safety buffer, i.e., the minimum arm-object distance below which penalties are applied, and the  $\hat{\cdot}$  notation indicates the use of a model that approximates the future state of the obstacle and the arm and its future actions.

To understand this, note that while  $\min_{1 \leq k < |S_i|} cd(\hat{s}_{t,h,n}^{(i,k)}, \hat{o}_{t,h,n}) \rightarrow B$  from above,  $f_{mask} = 0$ , so the term  $\hat{c}_{dyn}$  we added is 0 (i.e., "masked"). However when  $cd(i, j) < B$  (i.e. the distance buffer is violated) then  $f_{mask} \rightarrow 1$  as  $cd(i, j)$  approaches 0.

### B. From Dynamic Obstacles to Arms

Two difficulties of dynamic obstacles are estimating their trajectories and performing real-time collision checking (where the latter is also required for static obstacles). However, in our case, each arm has good approximate knowledge of its expected commands over the next  $H$  steps  $\{\pi_{\phi_{t,h}}\}_{h=0}^{H-1}$ , along with its dynamics model  $\hat{f}_d$ . We use this to extract their estimated sphere trajectories. See Alg. 1, line 10. More specifically, recall that STORM maintains a distribution over control signals for each time step  $t$ . We use the distribution's mean to generate a trajectory, (i.e., as done in trajectory sampling, but with  $\varepsilon_{t,h} = 0$ ). For each horizontal step  $h$ , each arm generates a set of spheres,  $S_{t,h}$ , that covers its position in workspace at step  $h$ , and sends it to other arms. The other arms treat these sphere sets as descriptions of dynamic obstacles (as explained above) and integrate them into their cost computation.

Note that the total work to compute collisions for robot  $i$  with all other robots  $j$  at step  $t$  corresponds to the total number of signed distance queries (i.e.  $cd(\cdot, \cdot)$ ) between each sphere of robot  $i$  and each sphere of robot  $j$ , given by

$$N_Q = \sum_{n=1}^N \sum_{h=0}^{H-1} \sum_{\substack{j=1 \\ j \neq i}}^{|A|} |S^{(i)}| \cdot |S^{(j)}|.$$

We leverage the GPU to parallelize this, computing

$\|\text{ctr}(s_1) - \text{ctr}(s_2)\| - (r_1 + r_2)$ . #center position, radius for every arm sphere and obstacle sphere, effectively computing this in  $\mathcal{O}(1)$ , since these are independent computations.

Another problem arises when arms need to reach or pass through similar positions. A large goal cost that dominates the collision cost is likely to cause the arms to collide. A large collision cost is likely to cause a deadlock, as both arms would be discouraged from reaching the desired position.

To address such potential deadlocks, we apply a multiplicative factor to the earlier definition of  $\hat{c}_{dyn_{t,h,n}}^{(i)}$ :

$$\hat{c}_{dyn_{t,h,n}}^{(i)} := \sum_{1 \leq j (\neq i) \leq |A|} \alpha_t^{(i,j)} f_{mask}(cd(\hat{a}_{t,h,n}^{(i)}, \hat{a}_{t,h}^{(j)}), B)$$

where

$$\alpha_t^{(i,j)} := \left( \frac{d_p(p_t^{ee_i}, g_i)}{d_p(p_t^{ee_j}, g_j)} \right)^\tau$$

$\alpha_t^{(i,j)}$  induces smooth prioritization (at time  $t$ ) of one robot over the other based on its relative distance to its goal.

More specifically,  $\alpha_t^{(i,j)}$  prioritizes the robot that is closer to its target. While different prioritization rules can be used for symmetry-breaking, depending on the overall goal (e.g [25]), following [7], our choice is motivated by the fact that a robot closer to its goal can more quickly attain it, leading to more immediate reward, and typically to eventually freeing up the region.

Notice also that the lower  $\alpha_t^{(i,j)}$  the higher  $\alpha_t^{(j,i)}$ . Hence, the more "aggressive"  $i$  is, the more "cautious"  $j$  will be. The degree to which this holds is determined by the exponent  $\tau$ , in  $\alpha_t^{(i,j)}$ , which we refer to as the *trust* parameter. It serves to amplify or de-amplify the effect of  $\alpha_t^{(i,j)}$ , which determines by how much the robot with the higher priority is allowed to ignore the other robot and vice versa. Thus, the higher  $\tau$ , the more the closer robot can ignore the other, and "trust" that the other robot will place greater weight on avoiding collisions with it. With 0 trust, i.e.,  $\tau = 0$ , we have  $\alpha_t^{(ij)} = 1$ , which effectively cancels prioritization.

### C. The MR-STORM Algorithm

The pseudo-code executed in MR-STORM by each robot appears in Algorithm 1 below. Changes from the original single-robot STORM algorithm are emphasized in red.

In MR-STORM, we assume robots are running the very same algorithm concurrently and asynchronously, and that each robot executes the control-loop until some stopping condition (like "timeout"), halts it. Let  $i$  be a general robot index. First, robot  $i$  writes its sphere-radii to a shared array  $r_{board}$  (line 1). On every step before optimization starts, the robot senses the robot-environment state (joints, obstacles, etc., line 3) and "shifts-left" the solution from the previous step – a standard step in STORM and other fixed horizon MPC methods, i.e., the previous step  $h$  is not step  $h - 1$ . This results in an  $H - 1$  step policy, which is extended to step  $H$  by replicating its last step. Then  $K$  (a typically small hyperparameter) policy-optimization steps are taken (line 5). On each optimization step,  $N$  candidate control sequences are sampled from the shifted policy;  $N$  rollouts are generated using the dynamics model; and the control distribution is updated once using the resulting costs (as described at eq. 4). In this step, we use the modified cost function- Equation 6

**Algorithm 1** MR-STORM: Agent  $i$ 's Control Generation Loop

**Require:**  $\theta_0$

**Parameters:**  $H, N, K$

```

1:  $r_{board}[i] \leftarrow \{r^{(i,j)}\}_{j=1}^{|S^{(i)}|}$ 
2: for  $t = 1 \dots T$  do
3:    $x_t \leftarrow \text{GETSTATE}()$ 
4:    $\pi_\theta \leftarrow \text{SHIFT}()$ 
5:   for  $i = 1 \dots K$  do // Optimization
6:      $u \leftarrow \text{SAMPLECONTROLS}(\pi_{\phi_t}, H, N)$ 
7:      $\hat{x}, \hat{c}, \hat{q} \leftarrow \text{GENERATEROLLOUTS}(x_t, H)$ 
8:      $\phi_t \leftarrow \text{UPDATEDISTRIBUTION}(\hat{c}, u)$ 
9:   end for
10:   $\pi_{board}[i] \leftarrow (\{FK(\hat{f}_d(\bar{\pi}_{\phi_t})_h)\}_{h=0}^{H-1}, d_p(p_t^{ee_i}, g_i))$ 
11:   $u_t \leftarrow \text{NEXTCOMMAND}(u, \hat{c})$ 
12:  EXECUTE( $u_t$ )
13: end for

```

using the most recent shared position estimates posted by other robots. (In step  $t = 1$ , such estimates are not yet available, and the arms ignore each other.) The policy can be represented as acceleration, velocity, or position commands. We use acceleration commands. After the optimization step, the robot applies the approximated dynamics model  $\hat{f}_d$  to the new policy to estimate its joint positions over time. Then, it applies forward-kinematics to these positions to get  $\{\hat{p}(s^{(i,j)})_{t,h}\}_{h=0,j=1}^{H-1,|S^{(i)}|}$ , i.e., sphere center position estimates over the horizon. It writes them to a shared array  $\pi_{board}$ , along with its goal error  $d_p$  to be used by other robots for computing  $\alpha_t^{(i,j)}$ . Finally, it executes the first action from the lowest-total-cost rollout (line 11 - 12).

## V. EMPIRICAL EVALUATION

### A. Setup

We evaluate our proposed method across a range of scenarios on goal achievement and collision avoidance. Experiments were conducted in NVIDIA's Isaac Sim V4.5 [8] to ensure realistic simulation conditions, on an 8-core CPU AMD® EPYC™ 7302 with 48 GB of RAM, and a single NVIDIA® RTX™ 4090 GPU, running Linux(Rocky). We note that lower-cost setups (32 GB RAM, NVIDIA® RTX™ 4060) produced similar results.

We tested the algorithms on four multi-arm manipulation tasks: *goal reaching easy*, *goal reaching hard*, *goal following*, and *bin-loading*, described below. Each task focuses on different aspects of MRMP. For each of the four task categories, 30 concrete tasks, which we also refer to as *environments*, were generated, 6 for each difficulty level. One trial was conducted for each environment. Within each level, environments differed by the goal positions used, which were sampled randomly. The same environments (with their goal choices) were used to test all algorithms.

We used  $N = 4$  arms and a popular 6-DOF arm platform *UR5e™* (reach=85cm) with a magnetic head in order to focus specifically on motion planning for the arms. In all trials,

the arms were positioned in the corners of a  $1m^2$  square, as shown in Fig 1A. Trials were halted after  $T_{max} = 500$  simulation steps, equivalent to  $\approx 8.33$  simulated seconds. Next, we describe each task's experimental setup in detail.

*a) Reaching:* When the trial starts, a random goal for each arm is sampled. When the arm reaches its goal (with error tolerance of 5cm) or when 1.0 (simulated) seconds have passed, the arm's goal changes. This task is divided into two equal sub-groups of 30 environments each: *A* (easy) and *B* (hard). In *reaching-easy*, goals are sampled around the arms. In this setup, the arms have almost no interaction with each other, which serves as a simple base case to examine the impact of coupled vs. decoupled computations. In *reaching-hard*, the goal positions are sampled around the midpoint between the arm and the center of the square, greatly increasing the potential for collisions. In both cases, the environment contains stationary and dynamic cuboid obstacles of different sizes (see Fig 1B,C). Dynamic obstacles move at a constant velocity into the work area. The arms have no prior information on the obstacles and their velocities, but can detect their current position. The five difficulty levels correspond to the number of obstacles introduced.

*Reaching-hard* is particularly challenging because the arms must react quickly to goal changes. Since their path undergo major changes every one second or less, it is much less predictable to the other arms. While the obstacles, especially the dynamic ones, greatly constrain free-space.

*b) Following:* Each trial starts by providing each arm with an initial goal pose, somewhere around it, similarly to goal positions used in *reaching-easy*. The targets move with constant velocity in an arbitrary direction and the arms must track it. When a target drifts too far from the arm, we reset it. As in the reaching tasks, the five difficulty levels differ in the number of obstacles. This task is used to evaluate the ability of the arms to perform tasks that have dynamic goals (e.g., cleaning a table or wiping a board) in the context of additional arms with a similar task.

*c) Bin Loading:* A bin with 4 cells is placed in the center of the square. See Fig 1A. Each arm has a fixed picking spot behind it. When the task begins, each arm has the goal of reaching its picking spot, where it picks, using its magnetic head, an object. Then, one of the four target cells is sampled as the arm's new goal, and the arm must carry the object to the cell's dropping point, which is 35 cm above its center. The different difficulty levels correspond to the number of arms that might need to drop an object concurrently. For  $l = 1, 2$ , at each point in time, one arm (respectively two) receives a cell area as a target. For  $l = 3$ , all arms can receive a bin cell as their goal, concurrently, but the cells must be different. For  $l = 4$ , only 2 arms can access the bin area concurrently, but they may receive the same target cell. For  $l = 5$ , all arms can get any bin cell concurrently as their goal, leading to a very challenging scenario. This task highlights high workspace overlap, where robots are extremely prone to inter-robot collisions, and is motivated by factory object-sorting scenarios.

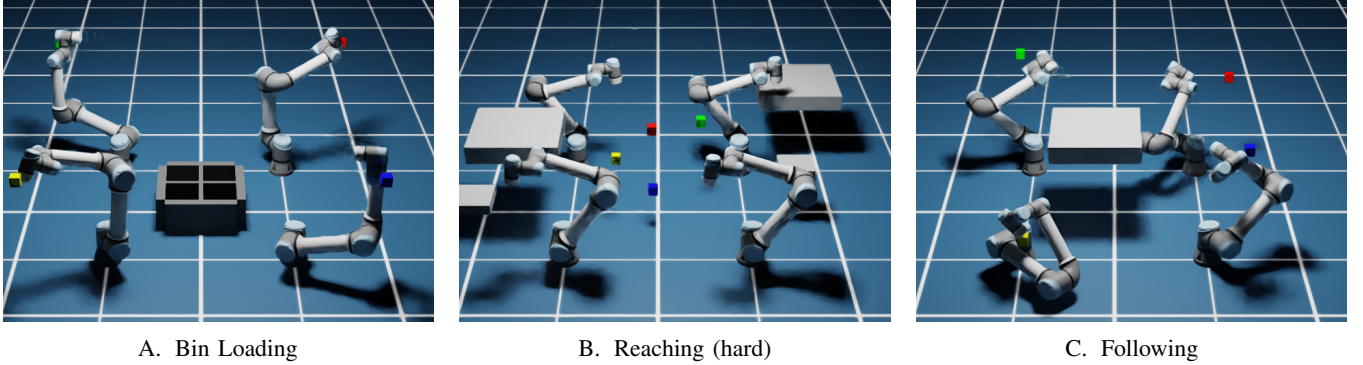


Fig. 1: Tasks Setups. A. Bin-Loading initial state. Colored cubes: picking positions. B. Reaching-Hard at initial state, level 5. Cuboids are dynamic and static obstacles. C. Following task, level=2. (one obstacle). Goals are mostly around the arms.

### B. Metrics, Baselines, Reporting

a) *Metrics*: For each environment, we record a collision and a task-specific score. The collision score is the number of steps, out of 500, in which any arm was in collision with another arm or the environment. The task-specific score for *reaching-hard* and *easy* is the total number of goals reached by  $T_{\max}$  by all arms. For *following* it is the mean end-effector positional error over arms and time, i.e.,

$$\overline{\text{err}}_f(t_r) = \frac{1}{T_{\max}} \sum_{t=1}^{T_{\max}} \frac{1}{|A|} \sum_{i \in A} d_p(p_t^{ee_i}, p_t^{g_i}),$$

For *bin-loading*: it is the total number of objects dropped in the bin by all arms.

b) *Algorithms Tested*: We compared three variants of our algorithm, MR-STORM (MRS for short). In all versions we used:  $H = 40$ ,  $w_d = 5000$ ,  $B = 0.3$  and  $\tau = 3$  (except where noted), with all other parameters set to their default value in the cuRobo library [19].

**MRS(400,5)**: MR-STORM with  $N = 400$  rollouts, and  $K = 5$  optimization iterations.

**MRS(400,1)**: MR-STORM with  $N = 400$  rollouts, and  $K = 1$ . Fewer optimization steps enable a higher control frequency.

**MRS-(400,1)**: MRS(400,5) with  $\tau = 0$ , i.e., with prioritization removed, in order to study its effect.

We compared these with other SOTA arm-specific, GPU-based, parallel compute, motion planners.

**CC(500), CC(1000)**: cuRobo is the SOTA algorithm of this type. We applied it to the coupled system, i.e., it controls all four arms. Two versions were tested with  $N_{IK\text{seeds}} = 500, 1000$ . These are the two IK seed number values recommended in [19]-A.8. Position error tolerance of 5cm was used, similar to that used in the reactive planners.

**SC(400,5), SC(1600,5)**: These are two versions of STORM coupled, i.e., using a single controller for all arms.  $N = 400$  is used to match the per-arm rollout budget of MRS.  $N = 1600$  was selected to match the combined rollout budget of the four arms. All STORM specific parameters are identical to those used in MRS(400,5).

**SD(400,5): STORM Decentralized**. All arms use STORM,

treating each other as static obstacles without prioritization or communication.

At each time point, all methods had access to the current position of static and dynamic obstacles. SD also had access to the arm’s positions, but not to their velocities. In addition, MRS had access to the messages sent by the other robots, as described earlier.

c) *Reporting*: We use *paired, per-environment differences* relative to a fixed baseline – MRS(400,5) – to remove nuisance variation due to different environment difficulty levels [26]. For each environment  $e$  and algorithm  $a$ , we computed  $\Delta T_{a,e} = T_{a,e} - T_{b,e}$ , where  $T_{a,e}$  is the task score of algorithm  $a$  in this environment. Similarly, for collisions:  $\Delta C_{a,e} = C_{a,e} - C_{b,e}$ . We aggregated these within-environment, normalized differences across all 30 environments, (5 difficulty blocks  $\times$  6 environments). We report the mean  $\pm$  SD. (Confidence intervals are less appropriate in this setting of multiple difficulty levels.) We avoid data-dependent normalizations (e.g., dividing by the per-environment maximum across algorithms), following recommendations for multi-dataset algorithm comparisons [26].

We also report the average control frequency:

$$F_c = \frac{1}{T_{\max}} \sum_{t=1}^{T_{\max}} t_{\text{plan}}(t),$$

where  $t_{\text{plan}}(t)$  is the sum over all planning related operations at time  $t$  (i.e. rows 3 to 11 in Alg. 1). Higher frequency indicates better responsiveness.

## VI. RESULTS

Figure 2 contains 3 graphs describing the average normalized task and collisions scores for the four tasks. To complete the picture, the average absolute goal and collision score for MRS(400,5) appear on the top left of each. For *bin-loading* 6.5 with 2 collisions. For *following* 0.1 with 3 collisions. For *reaching-easy* 27.1 with 3 collisions and for *reaching-hard* 8 with 13 collisions. Then, focusing on the top three performers in terms of goal achievement, one from each algorithmic family. We provide mean and std goal and collision scores (normalized, as above) for each difficulty level.

A number of clear trends emerge. First, we see that the coupled solvers perform poorly. The two CC variants are the worst, and although the two SC are better, they still perform poorly. We attribute this general trend to the difficulty these algorithms have scaling up to the large number of DOF in the "combined" robot. For example, in *bin-loading*, CC finds solutions only in level 1, and in the other levels, where arms interact, it cannot. A key problem is that, often, it cannot find a collision-free path for all arms, jointly, whereas in the decoupled algorithm, an arm doesn't care about the other arms, and if it can achieve the goal, it will. Typically, eventually, the other arms will achieve the goal, e.g., as the arm moves to a new goal position or to the object picking area. Beyond the computational overhead, this is a poor method for handling dynamic obstacles, and CC is also less reactive: it generates the entire motion plan, executing it for multiple steps, replanning only when a new goal arrives. Second, we see that the dynamic prioritization scheme used by MRS is important to its performance: MRS-(5,400) (i.e., without prioritization) has consistently lower goal scores in all domains, except *following*, and slightly more collisions, too. Third, reviewing MRS(1,400), we see that the additional optimization iterations provide only minor improvement. The collision score is virtually the same, and the effect on the goal score is very small (especially in comparison to other algorithms). This is noteworthy because, as we see in Table I, its control frequency is much higher, similar the published frequency of STORM for a single arm [5].

Fourth, the best goal scores are consistently attained by SD, but with a huge safety cost in domains in which arms can interact with each other. For example, in *reaching-easy*, which features little interaction, it is the clear winner in Levels 1-3. But, as we move to Levels 4,5, and to *reaching-hard*, we pay a substantial price of collisions in over 20% of the steps! This holds true for levels 2-5 of bin-loading, where this figure jumps to 40% and in level 5 of *following*. Overall, we believe that the conclusion is clear (and intuitive): if arms do not interact with each other, there's no reason or value to path sharing information. A completely decoupled approach works well. However, if arms interact, then the safety price of SD is too large to consider it a viable option, and the MRS(5,400) or MRS(1,400) is the clear choice.

Finally, we also measured the control frequency of the algorithms. These are shown in Table I for the interesting algorithms. Differences between algorithms are minor, and what affects this most is the number of optimization steps.

Algorithm	Mean	Median	Std
MRS (400,1)	50.088	55.237	11.047
SC (400,5)	20.158	20.416	3.059
SD (400,5)	17.265	17.643	2.110
MRS (400,5)	15.404	14.528	3.718

TABLE I: Control frequencies over all environments. (N=120 for each of the algorithms).

## VII. SUMMARY

We described a modification of the STORM algorithm to the multi-arm setting using a modified cost function and distance-based prioritization. Extensive experimental evaluations in challenging simulated environments show that this algorithm offers the best performance subject to safety constraints.

## VIII. LIMITATIONS

Our work considers simulation data only due to a lack of access to multiple physical arms. However, much like similar recent papers on this topic [4], [23], we partially compensate for this with a varied and challenging set of simulated environments. Yet, future, real-world implementations are clearly desirable. The MPC-based approach is local, by definition, and hence does not guarantee optimality and completeness. Yet, we have not seen attempts to run complete and optimal algorithms in the type of challenging tasks described in this paper. Finally, the use of spheres to approximate obstacles may not be optimal, and meshes or point clouds should be considered.

## REFERENCES

- [1] "drrt\*: Scalable and informed asymptotically-optimal multi-robot motion planning," *Autonomous Robots*, vol. 44, no. 3–4, p. 443–467, Jan.
- [2] "Conflict-based search for optimal multi-agent pathfinding," *Artificial Intelligence*, vol. 219, pp. 40–66, 2015.
- [3] M. Erdmann and T. Lozano-Pérez, "On multiple moving objects," *Algorithmica*, vol. 2, no. 1–4, p. 477–521, Nov. 1987.
- [4] A. Tajbakhsh, L. T. Biegler, and A. M. Johnson, "Conflict-based model predictive control for scalable multi-robot motion planning," 2024.
- [5] M. Bhardwaj, B. Sundaralingam, A. Mousavian, N. D. Ratliff, D. Fox, F. Ramos, and B. Boots, "Storm: An integrated framework for fast joint-space model-predictive control for reactive manipulation," in *Proceedings of the 5th Conference on Robot Learning*, A. Faust, D. Hsu, and G. Neumann, Eds., vol. 164, 2022, pp. 750–759.
- [6] G. Williams, A. Aldrich, and E. Theodorou, "Model predictive path integral control: From theory to parallel computation," *Journal of Guidance, Control, and Dynamics*, vol. 40, pp. 1–14, 01 2017.
- [7] D. Mateu-Gómez, F. J. Martínez-Peral, and C. Pérez-Vidal, "Multi-arm trajectory planning for optimal collision-free pick-and-place operations," *Technologies*, vol. 12, no. 1, 2024.
- [8] NVIDIA, "Isaac Sim." [Online]. Available: <https://github.com/isaac-sim/IsaacSim>
- [9] L. E. Kavraki, P. Švestka, J.-C. Latombe, and M. Overmars, "Probabilistic roadmaps for path planning in high dimensional configuration spaces," *IEEE Transactions on Robotics and Automation*, vol. 12, no. 4, pp. 566–580, 1996.
- [10] E. W. Dijkstra, "A note on two problems in connexion with graphs," *Numerische mathematik*, vol. 1, no. 1, pp. 269–271, 1959.
- [11] P. E. Hart, N. J. Nilsson, and B. Raphael, "A formal basis for the heuristic determination of minimum cost paths," *IEEE Transactions on Systems Science and Cybernetics*, vol. 4, no. 2, pp. 100–107, 1968.
- [12] A. T. Stentz, "Optimal and efficient path planning for partially-known environments," in *Proceedings of (ICRA) International Conference on Robotics and Automation*, vol. 4, May 1994, pp. 3310 – 3317.
- [13] S. M. LaValle, "Rapidly-exploring random trees : a new tool for path planning," *The annual research report*, 1998.
- [14] S. Karaman and E. Frazzoli, "Sampling-based algorithms for optimal motion planning," 2011.
- [15] N. Ratliff, M. Zucker, J. A. Bagnell, and S. S. Srinivasa, "Chomp: Gradient optimization techniques for efficient motion planning," in *2009 IEEE International Conference on Robotics and Automation*. IEEE, 2009, pp. 489–494.
- [16] M. Kalakrishnan, S. Chitta, E. Theodorou, P. Pastor, and S. Schaal, "Stomp: Stochastic trajectory optimization for motion planning," in *2011 IEEE International Conference on Robotics and Automation*, 2011, pp. 4569–4574.

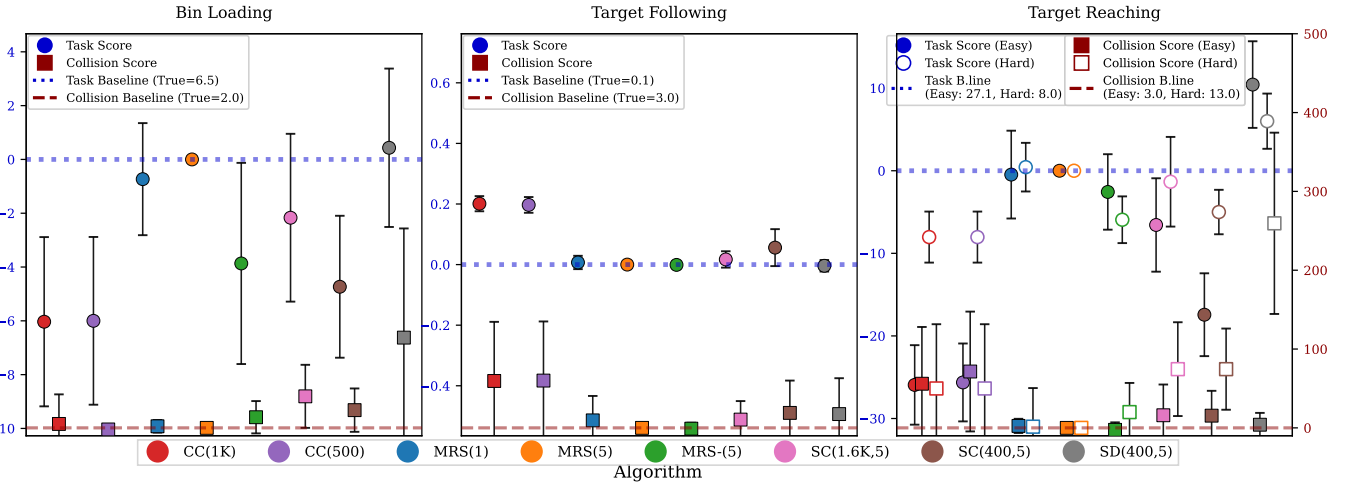


Fig. 2: Average normalized task (circles) and collision (square) scores with one standard deviation. Color code on the bottom. Task score scale on the left. Collision to the left. Dotted lines are the 0 baseline, representing MRS(400,5). For reaching: full circle/square for *easy* and empty for *hard*.

TABLE II: Results for Task Bin-Loading. Each cell: Task mean $\pm$ Task std, Collision mean $\pm$ Collision std.

Algorithm	Level 1	Level 2	Level 3	Level 4	Level 5
CC(1000)	-0.8 $\pm$ 1.8, 0.0 $\pm$ 0.0	-6.5 $\pm$ 1.5, 0.0 $\pm$ 0.0	-9.0 $\pm$ 0.6, -1.0 $\pm$ 1.5	-6.3 $\pm$ 1.4, 33.5 $\pm$ 81.5	-7.5 $\pm$ 1.9, -8.5 $\pm$ 10.5
SC(1600,5)	1.0 $\pm$ 2.7, 4.0 $\pm$ 10.0	-1.3 $\pm$ 2.0, 46.5 $\pm$ 58.5	-5.0 $\pm$ 3.3, 80.5 $\pm$ 20.0	-2.3 $\pm$ 2.4, 24.0 $\pm$ 28.5	-3.2 $\pm$ 2.1, 45.5 $\pm$ 25.0
SD(400,5)	1.2 $\pm$ 2.3, 0.0 $\pm$ 0.0	0.5 $\pm$ 3.0, 109.0 $\pm$ 117.0	0.7 $\pm$ 2.8, 126.5 $\pm$ 133.0	-0.2 $\pm$ 3.7, 143.0 $\pm$ 156.0	0.0 $\pm$ 3.6, 194.5 $\pm$ 176.5

TABLE III: Results for Task Reaching-Easy. Each cell: Task mean $\pm$ Task std, Collision mean $\pm$ Collision std.

Algorithm	Level 1	Level 2	Level 3	Level 4	Level 5
CC(1000)	-28.0 $\pm$ 5.2, 0.0 $\pm$ 0.0	-26.5 $\pm$ 2.9, 22.5 $\pm$ 55.5	-26.8 $\pm$ 2.7, 22.5 $\pm$ 55.5	-25.7 $\pm$ 4.4, 85.0 $\pm$ 61.5	-22.7 $\pm$ 7.3, 150.0 $\pm$ 48.0
SC(1600,5)	-4.8 $\pm$ 2.1, 0.0 $\pm$ 0.0	-7.0 $\pm$ 4.6, 0.0 $\pm$ 0.0	-5.0 $\pm$ 2.4, 0.0 $\pm$ 0.0	-3.5 $\pm$ 6.0, -1.0 $\pm$ 2.0	-12.5 $\pm$ 7.6, 81.5 $\pm$ 49.5
SD(400,5)	11.2 $\pm$ 5.5, 0.0 $\pm$ 0.0	11.8 $\pm$ 5.9, 0.0 $\pm$ 0.0	11.0 $\pm$ 5.6, 0.0 $\pm$ 0.0	10.5 $\pm$ 3.7, 4.0 $\pm$ 12.5	7.7 $\pm$ 6.1, 17.0 $\pm$ 30.5

TABLE IV: Results for Task Reaching-Hard. Each cell: Task mean $\pm$ Task std, Collision mean $\pm$ Collision std.

Algorithm	Level 1	Level 2	Level 3	Level 4	Level 5
CC(1000)	-10.3 $\pm$ 1.6, -18.5 $\pm$ 33.0	-8.5 $\pm$ 3.1, -3.0 $\pm$ 5.0	-7.7 $\pm$ 4.3, -9.0 $\pm$ 15.0	-8.0 $\pm$ 2.7, 135.5 $\pm$ 4.5	-5.7 $\pm$ 1.9, 144.5 $\pm$ 68.5
SC(1600,5)	1.0 $\pm$ 6.3, 78.5 $\pm$ 68.0	-2.3 $\pm$ 6.9, 74.5 $\pm$ 27.0	-1.7 $\pm$ 5.6, 72.5 $\pm$ 38.5	-3.2 $\pm$ 2.5, 88.0 $\pm$ 53.5	-0.5 $\pm$ 5.7, 58.0 $\pm$ 102.0
SD(400,5)	6.2 $\pm$ 3.8, 318.0 $\pm$ 102.5	6.3 $\pm$ 5.5, 296.0 $\pm$ 106.0	6.5 $\pm$ 3.7, 279.0 $\pm$ 73.0	5.0 $\pm$ 1.5, 224.5 $\pm$ 95.5	6.0 $\pm$ 1.4, 179.0 $\pm$ 157.5

TABLE V: Results for Task Following. Each cell: Task mean $\pm$ Task std, Collision mean $\pm$ Collision std.

Algorithm	Level 1	Level 2	Level 3	Level 4	Level 5
CC(1000)	0.2 $\pm$ 0.0, 0.0 $\pm$ 0.0	0.2 $\pm$ 0.0, 0.0 $\pm$ 0.0	0.2 $\pm$ 0.0, 0.0 $\pm$ 0.0	0.2 $\pm$ 0.0, 137.0 $\pm$ 1.5	0.2 $\pm$ 0.0, 161.0 $\pm$ 19.5
SC(1600,5)	0.0 $\pm$ 0.0, 0.0 $\pm$ 0.0	0.0 $\pm$ 0.0, 0.0 $\pm$ 0.0	0.0 $\pm$ 0.0, 0.0 $\pm$ 0.0	0.0 $\pm$ 0.0, 0.5 $\pm$ 1.0	0.0 $\pm$ 0.1, 52.5 $\pm$ 23.5
SD(400,5)	-0.0 $\pm$ 0.0, 0.0 $\pm$ 0.0	0.0 $\pm$ 0.0, 86.5 $\pm$ 69.5			

- [17] G. Williams, A. Aldrich, and B. Boots, “Information theoretic mpc for model-based reinforcement learning,” University of Washington, Tech. Rep., 2018.
- [18] M. S. Gandhi, B. I. Vlahov, J. Gibson, G. Williams, and E. A. Theodorou, “Robust model predictive path integral control: Analysis and performance guarantees,” *IEEE Robotics and Automation Letters*, vol. 6, no. 2, pp. 1423–1430, apr 2021.
- [19] B. Sundaralingam, S. K. S. Hari, A. Fishman, C. Garrett, K. V. Wyk, V. Blukis, A. Millane, H. Oleynikova, A. Handa, F. Ramos, N. Rathliff, and D. Fox, “eurobo: Parallelized collision-free minimum-jerk robot motion generation,” 2023.
- [20] A. Orthey, C. Chamzas, and L. E. Kavraki, “Sampling-based motion planning: A comparative review,” *Annual Review of Control, Robotics, and Autonomous Systems*, vol. 7, no. Volume 7, 2024, pp. 285–310, 2024.
- [21] D. Halperin, L. E. Kavraki, and K. Solovey, “Robotics,” in *Handbook of Discrete and Computational Geometry*, J. E. Goodman, J. O’Rourke, and C. D. Tóth, Eds. Boca Raton, NY: CRC Press, 2017.
- [22] D. Silver, “Cooperative pathfinding,” *Proceedings of the AAAI Conference on Artificial Intelligence and Interactive Digital Entertainment*, vol. 1, no. 1, pp. 117–122, Sep. 2021.
- [23] I. Solis, R. Sandström, J. Motes, and N. M. Amato, “Representation-optimal multi-robot motion planning using conflict-based search,” 2020.
- [24] J. van den Berg, S. Guy, M. Lin, and D. Manocha, *Reciprocal n-Body Collision Avoidance*, 04 2011, vol. 70, pp. 3–19.
- [25] J. van den Berg and M. Overmars, “Prioritized motion planning for multiple robots,” in *2005 IEEE/RSJ International Conference on Intelligent Robots and Systems*, 2005, pp. 430–435.
- [26] J. Demšar, “Statistical comparisons of classifiers over multiple data sets,” *Journal of Machine Learning Research*, vol. 7, pp. 1–30, 2006.